Dissipative particle dynamics simulation of flow generated by two rotating concentric cylinders: Boundary conditions

S. Haber,[1,*] N. Filipovic,[2,3] M. Kojic,[2,3] and A. Tsuda[3]
[1]*Technion-Israel Institute of Technology, Haifa, Israel*
[2]*University of Kragujevac, Kragujevac, Serbia*
[3]*Harvard School of Public Health, Harvard University, Boston, Massachusetts, USA*
(Received 5 December 2005; revised manuscript received 19 July 2006; published 3 October 2006)

The dissipative particle dynamics (DPD) method was used to simulate the flow in a system comprised of a fluid occupying the space between two cylinders rotating with equal angular velocities. The fluid, initially at rest, ultimately reaches a steady, linear velocity distribution (a rigid-body rotation). Since the induced flow field is *solely* associated with the no-slip boundary condition at the walls, we employed this system as a benchmark to examine the effect of bounce-back reflections, specular reflections, and Pivkin-Karniadakis no-slip boundary conditions, upon the steady-state velocity, density, and temperature distributions. An additional advantage of the foregoing system is that the fluid occupies inherently a finite bounded domain so that the results are affected by the prescribed no-slip boundary conditions only. Past benchmark systems such as Couette flow between two infinite parallel plates or Poiseuille flow in an infinitely long cylinder must employ artificial periodic boundary conditions at arbitrary upstream and downstream locations, a possible source of spurious effects. In addition, the effect of the foregoing boundary conditions on the time evolution of the simulated velocity profile was compared with that of the known, time-dependent analytical solution. It was shown that bounce-back reflection yields the best results for the velocity distributions with small fluctuations in density and temperature at the inner fluid domain and larger deviations near the walls. For the unsteady solutions a good fit is obtained if the DPD friction coefficient is proportional to the kinematic viscosity. Based on dimensional analysis and the numerical results a universal correlation is suggested between the friction coefficient and the kinematic viscosity.

DOI: 10.1103/PhysRevE.74.046701 PACS number(s): 47.11.−j, 47.10.−g, 47.11.St

I. INTRODUCTION

The dissipative particle dynamics (DPD) method to simulate flow fields of complex fluids was first suggested by Hoogerbrugge and Koelman [1] and in revised form by Espanol and Warren [2]. According to this method, the fluid is divided into mesoscale particles so that each particle contains a large number of molecules, but is still much smaller than the dimensions of the containing vessel. Based on concepts prevalent in molecular dynamics (MD) theory a Langevin equation was postulated by which the motion of the fluid particles can be calculated. The forces exerted on every particle by its neighbors, which are within a prescribed distance r_c (radius of influence) from it, are normally divided into three categories: conservative repulsive forces that can be derived from a potential function, dissipative forces that stem from viscous friction generated by the relative translational motion of adjacent particles, and random forces that may be significant due to the mesoscale dimension of the particles.

One of the controversial, unsettled aspects in DPD modeling relates to the formulation of the proper no-slip conditions near a rigid wall. The Lee-Edwards method [3], and its nonequilibrium molecular dynamics (NEMD) modification [4], in essence, circumvented the problem of how to avoid particles that can both penetrate and slide along rigid walls. Their ingenious suggestion that worked quite well for Couette flows, in which particles penetrating one wall should be reintroduced at the other wall, can hardly be qualified as a condition that should be applied *locally* at any rigid wall in more complex flow systems. A more advanced suggestion was to freeze regions of fluid near the rigid wall (Hoogerburgge and Koelman [1], Boek *et al.* [5], Hong [6]). This, however, resulted in possible particle penetration through the walls due to the "soft" conservative potential (Revenga *et al.* [7]). To avoid such aphysical results various methods have been suggested that combine the freezing particle layer near the wall with specular, bounce-back or Maxwellian reflection of a particle reaching a rigid wall (e.g., [1,7]). More recently, Pivkin and Karniadakis [8] suggested combining the above with an augmented conservative force at the rigid wall.

To the best of our knowledge, for *all* previous systems for which different boundary conditions were examined (investigating their effect on flow, density, and temperature distributions), open, unbounded flow systems were employed. Frequently, fully developed Couette and Poiseuille flows were used as benchmarks. Despite the fact that these flow systems possess simple analytic solutions, they suffer from a serious drawback. The infinite extent of the flow field, in the upstream and downstream directions, poses a serious numerical problem. One is forced to limit the solution domain and subject the flow field to additional *artificial* periodic boundary conditions at *arbitrary* upstream and downstream locations. Thus investigations seeking to obtain the *net* effect of a given set of boundary conditions at rigid walls are more likely to obtain the combined effect of the boundary conditions applied at the rigid walls and those assumed at the open ends of the flow.

*Corresponding author.

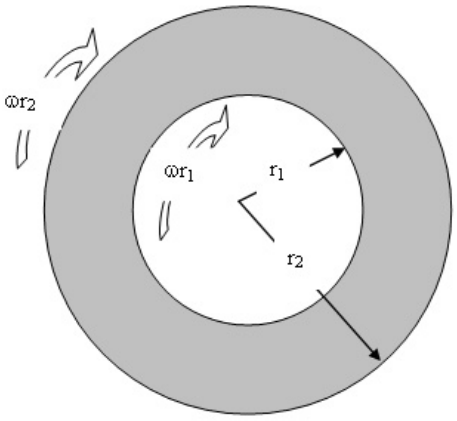

FIG. 1. The benchmark system (fluid occupies the space between two cylinders rotating with identical angular velocity ω).

We suggest employing a new benchmark system that consists of a fluid occupying the space between two concentric, rigid, infinitely long cylinders (see Fig. 1). The two-dimensional (2D) flow induced by the rotation of the cylinders results solely from the no-slip assumption. Thus, the system is excellently fit to address the question of how specular reflection, bounce-back reflection, and the Pivkin and Karniadakis (PK) boundary conditions affect the flow, density, and temperature fields. Importantly, as a completely 2D closed system, it does not suffer from the forgoing ambiguities associated with artificial boundaries and/or *ad hoc* boundary conditions as is the case of open systems. Indeed, we may also compare the transient DPD solutions with those known from continuum mechanics, a comparison that may yield the relation between the macroscopic kinematic viscosity of the fluid and the DPD friction coefficient.

Flekkoy and Coveney [9] and in particular Flekkoy *et al.* [10] have suggested to link the DPD and MD equations that govern the motion of the mesoscopic- and molecular-size particles, respectively (a bottom-up strategy). Thus the friction coefficient was linked to the dynamic viscosity η of a Newtonian fluid perceived as a continuum and the ratio between intersection length and distance between two interacting Voronoi cells. However, to reach closure it was still required to define constitutive relations prevailing at the continuum level (top-down strategy), as suggested by Espanol and Revenga [11]. In this article, we adopt the strategy initiated by Hoogerbrugge and Koelman [1] and further developed by Espanol and Warren [2] and Espanol [12]—namely, that the DPD equations governing the motion of identical, mesoscopic particles are *postulated*. The complementing multiparticle collision models (also known as stochastic rotation dynamics) introduced in Malevanets and Karpal [13,14], Marsh and Yeomans [15], Kikuchi *et al.* [16], and recently Webster and Yeomans [17] are not addressed in this paper.

II. METHOD

A. DPD equations of motion

During more than a decade, a considerable number of articles have focused on the proper formulation for the equations governing the different forces and how their *a priori* unknown parameters are related to the known phenomenological coefficients of the fluid. A widely accepted formulation for the equations of motion of a DPD particle is (e.g., Espanol and Warren [2], Groot and Warren [18], Novik and Coveney [19], Besold *et al.* [20], Pivkin and Karniadakis [8])

$$d\mathbf{r}_i = \mathbf{v}_i dt,$$

$$d\mathbf{v}_i = \sum_{j\neq i} \mathbf{F}_{ij} dt = \sum_{j\neq i} (\mathbf{F}_{ij}^C dt + \mathbf{F}_{ij}^D dt + \mathbf{F}_{ij}^R dt^{1/2}), \tag{1}$$

where $d\mathbf{r}_i$ and $d\mathbf{v}_i$ are the infinitesimal displacement and velocity change, measured relative to a Galilean coordinate system, that particle i undergoes during the time increment dt. The forces $\mathbf{F}_{ij}^C$, $\mathbf{F}_{ij}^D$, and $\mathbf{F}_{ij}^R$ are the conservative (repulsive), dissipative, and random forces (per unit mass of particle i) that particle j exerts on particle i, respectively, provided particle j is within the radius of influence r_c of particle i,

$$\mathbf{F}_{ij}^C = a_{ij}(1 - r_{ij}/r_c)\mathbf{e}_{ij},$$

$$\mathbf{F}_{ij}^D = -\gamma(1 - r_{ij}/r_c)^2(\mathbf{v}_{ij}\cdot\mathbf{e}_{ij})\mathbf{e}_{ij},$$

$$\mathbf{F}_{ij}^R = (2k_BT\gamma/m_i)^{1/2}(1 - r_{ij}/r_c)\xi_{ij}\mathbf{e}_{ij}. \tag{2}$$

Here a_{ij} is the maximum repulsion force per unit mass, r_{ij} is the distance between particles i and j, $\mathbf{e}_{ij}$ is a unit vector pointing in a direction from j to i, $\mathbf{v}_{ij}=\mathbf{v}_i-\mathbf{v}_j$ is the velocity of particle i relative to that of particle j, m_i is the mass of particle i, γ stands for the friction coefficient, k_B is the Boltzmann constant, T is the equilibrium temperature, and ξ_{ij} is a random number with zero mean and unit variance. In the case $r_{ij}>r_c$ particle j is assumed to exert no force on particle i. Notice that a "soft" interaction conservative force was employed here (used frequently in the past—e.g., [8,18,21,22]), that the dissipative and random forces that particle j exerts on particle i were assumed to depend upon the distance between these particles, that the dissipative force also depends upon a single component of the relative velocity between the particles $(\mathbf{v}_{ij}\cdot\mathbf{e}_{ij})$, and that the direction of all the foregoing forces is along the line connecting the centers of the two particles.

If we define the dimensionless variables

$$\hat{\mathbf{r}}_i = \mathbf{r}_i/r_c,$$

$$\hat{r}_{ij} = r_{ij}/r_c,$$

$$\hat{\mathbf{v}}_{ij} = \mathbf{v}_{ij}/v_T,$$

$$\hat{t} = tv_T/r_c, \tag{3}$$

where $v_T=(k_BT/m_i)^{1/2}$ is the thermal velocity of particle i, Eq. (1) possesses the following dimensionless form:

$$d\hat{\mathbf{r}}_i = \hat{\mathbf{v}}_i d\hat{t},$$

$$d\hat{\mathbf{v}}_i = \sum_{j\neq i} \frac{q_{ij} r_c}{v_T^2}(1-\hat{r}_{ij})\mathbf{e}_{ij}d\hat{t} - \frac{\gamma r_c}{v_T}(1-\hat{r}_{ij})^2(\hat{\mathbf{v}}_{ij}\cdot\mathbf{e}_{ij})\mathbf{e}_{ij}d\hat{t} + \left(\frac{2\gamma r_c}{v_T}\right)^{1/2}(1-\hat{r}_{ij})\xi_{ij}\mathbf{e}_{ij}d\hat{t}^{1/2}. \quad (4)$$

In case all particles have identical mass and all the a_{ij} coefficients are equal, Eq. (4) depends only on two dimensionless numbers

$$\hat{a} = a_{ij} r_c / v_T^2, \quad \hat{\gamma} = \gamma r_c / v_T. \quad (5)$$

Thus there is no need to assume that the trio—the mass of a particle m, $k_B T$, and r_c—are all unity, an assumption made in many previous studies. It is sufficient to assume that ν_T and r_c are equal to 1 and vary γ and a_{ij} to obtain different DPD fluids. (This would be equivalent to setting numerical values to the dimensionless variables $\hat{a}$ and $\hat{\gamma}$.)

The boundary conditions would introduce at least two additional dimensionless parameters

$$\hat{L} = L/r_c, \quad \hat{V}_W = V_W/v_T, \quad (6)$$

where L and V_w scale the macroscopic size of the system and the velocity of its wall, respectively.

More recently, Espanol [12] suggested that additional components to the dissipative and concomitant random forces be added. These included force components perpendicular to $\mathbf{e}_{ij}$ and the effect of particle rotation. The former is a natural extension based on simple tensorial considerations, and the latter stems from the finiteness of the particles. Based on MD theory Flekkoy and Coveney [9] and Flekkoy *et al.* [10] have also obtained that at the DPD mesoscale forces that are not collinear with $\mathbf{e}_{ij}$ exist. These modifications, however, have not thoroughly been tested, and their contribution to the solution accuracy is awaiting further exploration.

B. DPD boundary conditions

The no-slip condition at the rigid walls is examined employing the specular and bounce-back reflections and the Pivkin and Karniadakis [8] boundary condition. In Galilean-invariant notation, the *local* specular reflection is

$$\mathbf{v}_{Wj}^{+}\cdot\mathbf{n}_W = -\mathbf{v}_{Wj}^{-}\cdot\mathbf{n}_W,$$

$$\mathbf{v}_{Wj}^{+}\cdot(\mathbf{I}-\mathbf{n}_W\mathbf{n}_W) = \mathbf{v}_{Wj}^{-}\cdot(\mathbf{I}-\mathbf{n}_W\mathbf{n}_W), \quad (7a)$$

where $\mathbf{I}$ is the idem dyadic, the minus and plus superscripts denote velocities before and after collision with the wall, $\mathbf{v}_{Wj}$ stands for the velocity of particle j relative to the velocity of the wall, and $\mathbf{n}_W$ is a unit vector perpendicular to the wall. Thus only the normal component is reflected while the tangential components remain unaltered. Notice that if the velocity of the wall relative to an outside observer is $\mathbf{V}_W$ and that of particle j relative to the same observer is $\mathbf{v}_j$ Eq. (7a) transforms into

$$\mathbf{v}_j^{+}\cdot\mathbf{n}_W = -\mathbf{v}_j^{-}\cdot\mathbf{n}_W + 2\mathbf{V}_W\cdot\mathbf{n}_W,$$

$$\mathbf{v}_j^{+}\cdot(\mathbf{I}-\mathbf{n}_W\mathbf{n}_W) = \mathbf{v}_j^{-}\cdot(\mathbf{I}-\mathbf{n}_W\mathbf{n}_W). \quad (7b)$$

The bounce-back reflection in Galilean-invariant form is

$$\mathbf{v}_{Wj}^{+} = -\mathbf{v}_{Wj}^{-}, \quad (8a)$$

which transforms into

$$\mathbf{v}_j^{+} = -\mathbf{v}_j^{-} + 2\mathbf{V}_W \quad (8b)$$

for velocities measured relative to an outside observer.

Equations (7b) and (8b) are more frequently used in cases where the system includes several rigid walls moving with different velocities relative to the same observer (e.g., in Couette flow one plane is moving and the other is at rest relative to the same observer)

A comparison between the specular and the bounce-back methods demonstrates that if the no-slip, no-penetration conditions are *nearly* satisfied by the particle prior reaching the wall, both methods yield (surprisingly) almost similar results. This can easily be verified. Introduction of $\mathbf{v}_j^{-} \approx \mathbf{V}_W + \boldsymbol{\varepsilon}$, $|\boldsymbol{\varepsilon}| < 1$, into Eqs. (7b) and (8b) yields velocities after the encounter with the wall v_j^{+} that differ by order $\boldsymbol{\varepsilon}$ only.

The Maxwellian reflection method that was also used in the past (e.g., Revenga *et al.* [7,21]) assumed that the particles are randomly reflected back to the flow with a Maxwellian velocity distribution centered around the wall velocity. This boundary condition will not be examined in this paper.

In a recent paper Pivkin and Karniadakis [8] suggested a method to impose no-slip boundary conditions that includes a frozen layer of particles near the wall, bounce-back reflection, *and* modification of the maximum conservative force a_W for particles interacting with the particles positioned at the frozen layer. The flow system used as a benchmark consisted of a fluid moving under gravity in a conduit with a rectangular cross section. Hong [6] used two frozen layers and showed good result in planar Poiseuille and Couette flows.

III. NUMERICAL APPROACH

An interesting and practical question that was raised in the past (e.g., Groot and Warren [18], Peters [22], Vattulainen *et al.* [23], Jakobsen and Mouritsen [24]) refers to the magnitude of the time increment to be used in the numerical procedure. Clearly, Eqs. (4) and (6) may be examined to assess what should be the largest dimensionless time increment possible. It would depend on the three dimensionless parameters $\hat{a}$, $\hat{\gamma}$, and $\hat{V}_W$, which indeed are based upon four time scales: r_c/v_T (which was used here to scale the time), $1/\gamma$, v_T/a_{ij}, and r_c/V_W. The shortest time scale would determine the dimensional time increment, and in dimensionless time units this time increment would be divided by r_c/v_T. Thus

$$\Delta\hat{t} = 10^{-N}\min(1, v_T/\gamma r_c, v_T^2/a_{ij} r_c, v_T/V_W), \quad (9)$$

where N determines the accuracy of the numerical solution (say, $N=3$). Groot and Warren [18] have shown that numerical artifacts may exist if the time step (in our dimensionless scale) is larger than 0.1. Vattulainen *et al.* [23] and Jakobsen and Mouritsen [24] have encountered similar problems. We used the Verlet algorithm with a time increment $\Delta\hat{t}=10^{-4}$, which is a much smaller value.

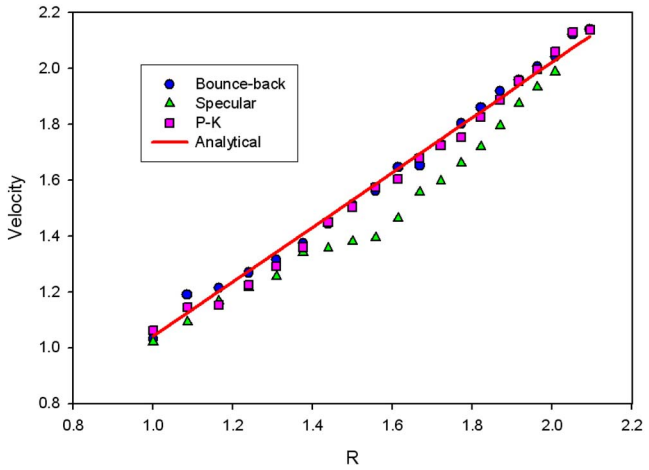

FIG. 2. (Color online) Velocity distribution for bounce-back, specular, and PK boundary conditions after 300 000 time steps.

Another important question relates to the total number of time steps required to reach steady state (if it exists). Continuum mechanics predicts that this time scales with L^2/ν where ν is the kinematic viscosity of the fluid. However, the evaluation of the kinematic viscosity in terms of the DPD parameters is still ambiguous and we shall address this important question in Sec. V. Notwithstanding, assuming that the kinematic viscosity is proportional to γ (see also a discussion by Flekkoy and Coveney [9] and Flekkoy *et al.* [10]) makes it possible to estimate the total number of time steps that are required to reach steady state:

$$N_{SS} = O(L^2/\nu\Delta t) = O(\hat{\gamma}\hat{L}^2/\Delta\hat{t}). \tag{10}$$

Throughout the paper we assumed that the 2D system contains 2520 DPD particles, the inner cylinder dimensionless radius is $r_1=5$ (in r_c units) and that of the outer cylinder is $r_2=10.683$ ($\hat{r}_2=r_2/r_1=2.1366$), the cylinders are rotating with the same angular velocity $\omega=0.2v_c/r_c$ (so that the dimensionless velocity of the inner cylinder is unity), and the fluid is assumed to be at rest initially (see Fig. 1). The wall is mimicked by frozen DPD particles moving with the exact velocity of the rotating cylinders. The velocity dependence on the radial coordinate and time was calculated by averaging the velocity of the particles inside 20 radial concentric rings during 2% of the total running time for $\hat{\gamma}=4.5$ and $\hat{a}=25$ (water, according to Groot and Warren [18]). Steady state was reached before completing 300 000 time steps.

IV. RESULTS

A. Comparison with the steady-state analytic solution

The following figures illustrate the velocity, density, and temperature distributions, employing the specular, bounce-back, and PK boundary conditions. A comparison is also carried out with the simple analytical steady-state solution.

Velocity distributions after 300 000 time steps, the time required to reach steady state, are shown in Fig. 2, employing the three different methods of no-slip boundary conditions. The results were evaluated against the analytical solution (solid line), a comparison that made it possible to calculate the mean error and standard deviation (Table I). This comparison shows that the bounce-back reflection method yields the best fit for the velocity distribution; the PK method is almost as good, but the worst results are obtained employing the specular reflection method. This conclusion reaffirms past observations made by Pivkin and Karniadakis [8] who compared the bounce-back and specular reflection methods. A comparison between Eqs. (7b) and (8b) may provide insight into why the bounce-back reflection is superior to the specular reflection method. The specular reflection method [Eq. (7b)] shows that the fluid particles are practically "unaware" of the cylinders' motion. In our case $\mathbf{n}\cdot\mathbf{V}_W$ vanishes identically; thus, the first equation of Eqs. (7b) simply requires that the reflected and incoming normal velocity components be equal in size and opposite in sign. The second equation of Eqs. (7b) pertains to the velocity components tangential to the wall. Again, there is no contribution of the wall velocity. Thus the only possible mechanism that may cause the *inner* fluid particles to be "aware" of the moving boundaries is through their interaction with the frozen particles positioned at the wall. The bounce-back method shows that particles approaching the walls are directly affected by the walls motion. The "law" for the component perpendicular to the wall is identical to that of the specular reflection. However, the equation for the tangential components shows that, in our case, $v_j^+(\text{tangential}) = -v_j^-(\text{tangential}) + 2\Omega_W R_W$, where Ω_W and R_W are the angular velocity and radius of the rotating cylinder, respectively. Thus the effect of the rotating wall is directly introduced through the boundary condition.

TABLE I. Velocity mean and standard deviation for all three boundary conditions.

Boundary condition after 300 000 time steps	Mean	Standard deviation
Bounce-back	-2.0916×10^{-3}	0.0275
Specular	0.0976	0.0528
PK	0.0119	0.0309

The density distribution along the radial direction is shown in Fig. 3. In all cases a strong aberration from uniformity exists near the walls due to the frozen layer assumption. If these particular locations are excluded, the standard deviation for all inner locations given in Table II shows that the specular reflection yields the worst results most likely due to the reasons discussed above, while bounce-back is slightly better. The PK method is superior in this case.

The temperature distribution along the radial direction is shown in Fig. 4. Again, a rather strong deviation from uniformity may exist near the walls, a likely outcome from the frozen layer assumption. Again, if we exclude the layers adjacent to the walls, the standard deviation based on internal layers (see Table III) is lowest for the bounce-back reflection method while the bounce specular reflection method yields the highest temperature fluctuations.

In addition, the results may also validate the stability of the analysis in relation to the size of the chosen time incre-

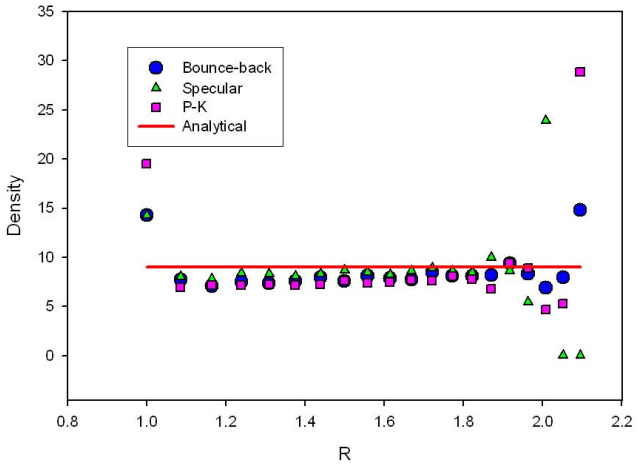

FIG. 3. (Color online) Density distribution for bounce-back, specular, and PK boundary conditions after 300 000 time steps.

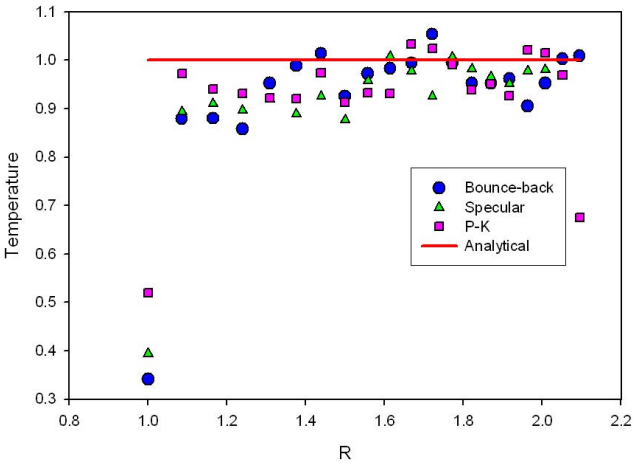

FIG. 4. (Color online) Temperature distribution for bounce-back, specular, and PK boundary conditions after 300 000 time steps.

ment ($\Delta t = 10^{-4}$). Indeed, Groot and Warren [18] found no error artifacts for a time step $\Delta t = 0.04$ and density $\rho = 3.0$. They used the deviations from the DPD thermostat kinetic temperature ($k_B T$) as a criterion for numerical instability emanating from large time steps. Comparison of our results presented in Fig. 4 with that of Groot and Warren [18] for the temperature distribution (using the same logarithmic scale) illustrates that our results can be considered stable.

B. Unsteady solutions

A comparison is carried out between the unsteady DPD solutions obtained by employing the three different sets of boundary conditions and the exact analytical solution of a fluid continuum described in the Appendix A. Figures 5–7 illustrate the instantaneous velocity profiles that exist before steady state is reached. Figure 5 was obtained for no-slip boundary conditions based on bounce-back reflections. The velocity radial distributions for six different times, which correspond to 50 000, 100 000, 150 000, 200 000, 250 000, and 300 000 time steps, are depicted. Note that the last two are already very close to steady state. A dimensionless time increment as large as 10^{-4} was used. Thus the figures show the velocity evolution for dimensionless DPD times $\hat{t} = 5, 10, 15, 20, (25, 30)$. The velocity profiles derived from the analytical solution (Appendix) are also shown for the physical dimensionless times $\hat{\tau} = 0.075, 0.15, 0.225, 0.3$, which correspond to the first four DPD times. Notice that this foursome is linearly related to the DPD times. Clearly, the DPD clock [Eq. (3)] and the physical clock [Eq. (A3)] have a different pace, but the results show that they tic at a uniform rate. Exact analytical velocity distributions for higher time values are not introduced since they are of limited value being so close to steady state. Excellent agreement is obtained for 100 000 time steps and higher, which corresponds to DPD times $\hat{t} > 10$. Only small aberrations are observed near the walls where the effect of the numerical bin size is more pronounced. For 50 000 time steps and lower, which corresponds to DPD dimensionless time $\hat{t} < 5$ and the associated physical dimensionless time $\hat{\tau} < 0.075$, the agreement is not as good. To enhance the DPD solution for such short times one probably needs to employ higher particle densities to capture more accurately the high wall shear rates that exist at the onset of the cylinders' motion.

Figure 6 portrays the velocity profiles obtained by the PK boundary conditions. The results are again very good for $\hat{t} > 10$, but no noticeable improvement can be observed if compared with the bounce-back reflection method. Figure 7 depicts the velocity profiles at identical times, provided the specular reflection method is employed. The results do not fit as well with the analytical solution, quite similar to our previous observations that dealt with the steady-state solutions.

TABLE II. Density mean and standard deviation for all three boundary conditions.

Boundary condition after 300 000 time steps	Mean	Standard deviation
Bounce-back	−1.1187	0.5466
Specular	−0.6950	0.9051
PK	−1.7594	0.9788

TABLE III. Temperature mean and standard deviation for all three boundary conditions.

Boundary condition after 300 000 time steps	Mean	Standard deviation
Bounce-back	−0.0403	0.0342
Specular	−0.0586	0.0425
PK	−0.0505	0.0412

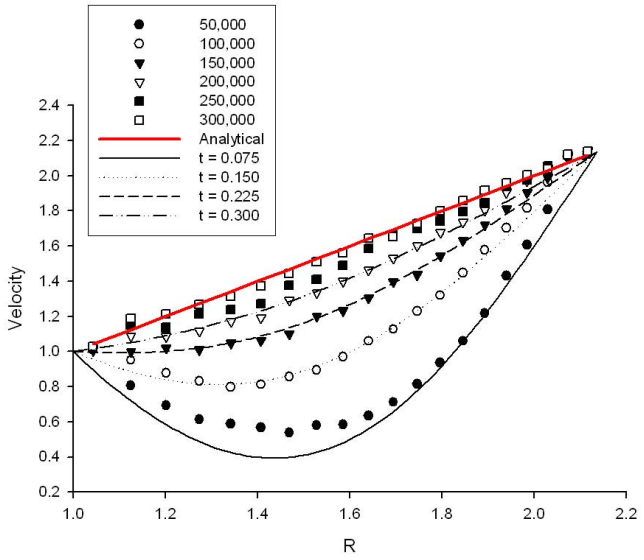

FIG. 5. (Color online) Unsteady velocity distribution for bounce-back boundary condition.

V. DISCUSSION: PHYSICAL PROPERTIES VERSUS THE DPD PARAMETERS

The all important question of how the known physical properties of fluids, such as viscosity, density, and temperature, correlate with the postulated DPD parameters such as γ, a_{ij}, and r_c is still widely debated (e.g., Revenga *et al.* [7]; see also our overview in the Introduction). Without that knowledge, no *useful* modeling of a real-life problem can be made.

The results obtained in Sec. IV B may help us explore the relation between the DPD friction coefficient and the fluid viscosity. We obtained that the DPD dimensionless time $\hat{t}=10$ corresponds to the physical dimensionless time $\hat{\tau}=0.15$.

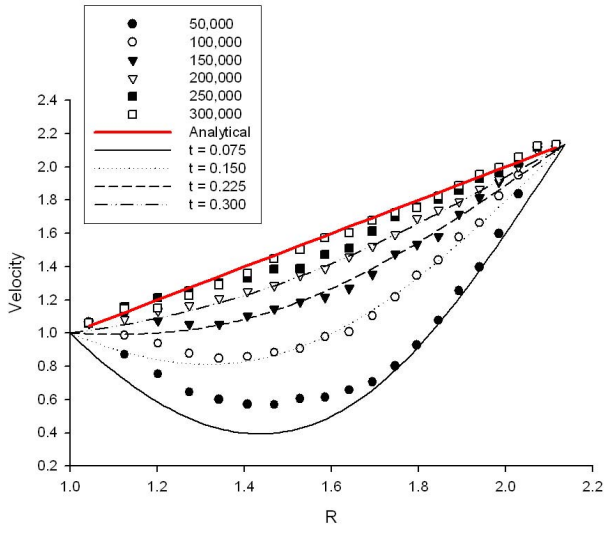

FIG. 6. (Color online) Unsteady velocity distribution for PK boundary conditions.

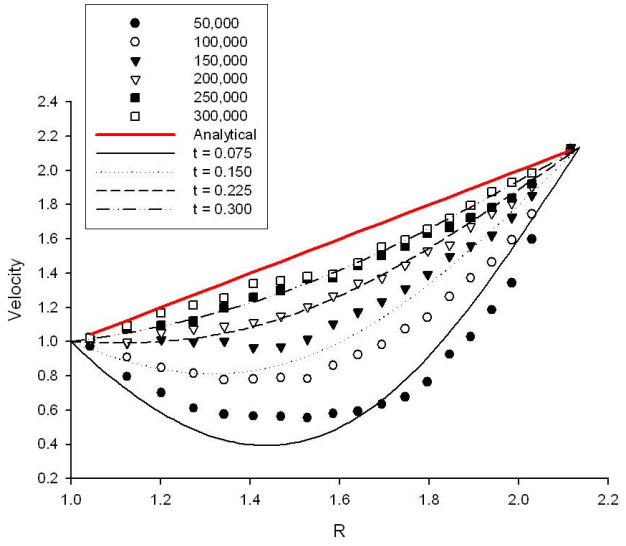

FIG. 7. (Color online) Unsteady velocity distribution for specular boundary condition.

Thus, a single DPD time unit is equivalent to 0.015 physical time units. Hence, for our *particular* example,

$$t = r_c/v_T = 0.015 r_1^2/\nu \tag{11a}$$

or

$$\nu = 0.015 r_1^2 v_T/r_c. \tag{11b}$$

We do not claim that this relation is general. To the contrary, the number 0.015 is not universal and would most generally depend on the DPD dimensionless parameter set $\hat{\gamma}$, $\hat{a}$, λ/r_c, r_1/r_c, the global geometrical parameter $R=r_2/r_1$, and the velocity ratio $\Omega r_1/v_T$. Thus a more general relation should be

$$\nu = f(\hat{\gamma},\hat{a},\lambda/r_c,R,r_1/r_c,\Omega r_1/v_T) r_1^2 v_T/r_c. \tag{12}$$

However, if the DPD equations have any merit, the kinematic viscosity cannot depend on the particular problem at hand—namely, on the size of the system[1] and the prescribed velocities at the boundaries; nor can it depend on the particular numerical choice of the number of particles per unit volume n that determines the mean distance between the particles λ. It can, however, depend on the phenomenological coefficients defining the DPD fluid: γ, a_{ij}, r_c, the fluid temperature, T, and its density $\rho=nm$, where m is the DPD's particle mass. The latter condition requires that only terms of the form $v_T/n^{1/2}=v_T\lambda^{3/2}$ be acceptable.

Under these conditions the function f in Eq. (12) is drastically simplified and must possess the following form:

[1]A word of caution: 2D and 3D systems may differ. Based upon MD theory, the Green-Kubo integrals over the autocorrelation functions associated with the transport coefficients in 2D systems do not converge (unlike the 3D cases) and thus are not well defined (see also discussions in Soddemann *et al.* [4], Ihle and Kroll [25], and Kikuchi *et al.* [16]).

$$f = \left(\frac{r_c}{r_1}\right)^2 g\left(\frac{\gamma r_c^{5/2}}{(k_B T/\rho)^{1/2}}, \frac{a_{ij} r_c^4}{k_B T/\rho}\right). \tag{13a}$$

And thus

$$\nu/\gamma r_c^2 = g\left(\frac{\gamma r_c^{5/2}}{(k_B T/\rho)^{1/2}}, \frac{a_{ij} r_c^4}{k_B T/\rho}\right), \tag{13b}$$

which solely depends on the phenomenological coefficients of the DPD model and the presumably known fluid density and temperature. If we further assume that the kinematic viscosity is proportional to the friction coefficient γ, Eq. (13) is further simplified:

$$\nu/\gamma r_c^2 = g\left(\frac{a_{ij} r_c^4}{k_B T/\rho}\right). \tag{14}$$

Equation (14) can also be rewritten in the following form employing only dimensionless DPD units:

$$\nu/r_c v_T = \hat{\gamma} g\left(\frac{\hat{a} r_c^3}{\lambda^3}\right). \tag{15}$$

How does this result compare with the existing literature?

Revenga *et al.* [7] suggested that the kinematic viscosity ν is related to the DPD parameters via the following formula:

$$\nu/\lambda v_T = 0.5[1/\xi + (3/40)s^2\xi], \quad \xi = \lambda\gamma/v_T, \tag{16}$$

where $\lambda = O(n^{-1/3})$ is the mean distance between the DPD particles of number density n and $s = r_c/\lambda$ (normally of order unity [Eq. (108) in Espanol [12]]). Thus, for given fluid of kinematic viscosity ν and particle number density n, the value of ξ is

$$\xi = 40\nu/(3\lambda v_T s^2) \pm \sqrt{[40\nu/(3\lambda v_T s^2)]^2 - 40/3s^2}.$$

Thus there are either two solutions or no physical solution if the term under the square root symbol is a negative number—namely, when

$$\lambda > (40/3)^{1/2}\nu/(3v_T s) \quad \text{or equivalently}$$
$$\text{if } n > O(40\nu^2\rho/3s^2 k_B T)^3. \tag{17}$$

At a glimpse, this is quite disturbing since it states that there is an upper bound for the number of DPD particles per unit volume that one is allowed to use. However, the upper bound for n indicated by inequality (17) for a real fluid—say, water or air at standard conditions—is 10^{36} or 10^{42} particles/m^3, respectively, larger than the number of molecules. Consequently, inequality (17) poses no practical limitation on the DPD scheme and two positive solutions may exist for very small or very large τ's, respectively,

$$\gamma \cong 0.5 k_B T n/\mu \tag{18a}$$

and

$$\gamma = (80/3)\nu/(\lambda s)^2 = (80/3)\nu/r_c^2, \tag{18b}$$

where μ is the fluid viscosity. The first solution is inversely proportional to the viscosity. It stems from momentum transfer caused by particle motion and based on the mean free path of the DPD particles. It is effectively negligible in our case and thus would not be applied. The second solution is proportional to the fluid viscosity. It stems from particle interactions that are highly significant at the mesoscale level addressed here.

Comparison of Eq. (14) with Eq. (18b) demonstrates that a match exists if g is constant. (In both cases the kinematic viscosity was assumed to be proportional to the friction coefficient γ.) For the example solved in this paper with DPD units, $\nu_T = r_c = 1$, $r_1 = 5$, and $\gamma = 4.5$, the value of ν obtained from Eqs. (11) and (14) is $\nu = 4.5$ $g = 0.015 \times 5^2$. Hence, assuming that $\hat{a}$ has no effect on the time evolution, we obtained that $g = 0.0833$ rather than $3/80 = 0.0375$, the value suggested in Revenga *et al.* [7].

VI. CONCLUSIONS

A benchmark model consisting of a fluid occupying the gap between two concentric cylinders rotating at equal angular velocities was utilized to explore the effect of the bounce-back, specular, and PK boundary conditions. The fluid flow field, density, and temperature radial distributions were examined at steady state and compared with the known linear analytic solutions. The comparison illustrated that the bounce-back boundary condition yielded the most accurate results, and agreement is best if the regions close to the walls are excluded. This deviation near the walls stems most probably from the fact that a layer of particles adjacent to the wall is assumed frozen. The unsteady DPD solution was also compared with the known analytic solution utilizing the bounce-back boundary condition. The results show a very good agreement for dimensionless times larger than 0.15 and agree with the ansatz that the fluid viscosity and the DPD friction coefficient are linearly related for mesoscale DPD particles. Based on dimensional analysis the following general relation was obtained:

$$\nu/r_c v_T = \hat{\gamma} g\left(\frac{\hat{a} r_c^3}{\lambda^3}\right).$$

If the function g assumes a constant value, independent of the parameter $\hat{a} r_c^3/\lambda^3$, and the numerical results for the unsteady case are employed, the following generalized correlation is obtained:

$$\nu/r_c v_T = 0.0833\hat{\gamma}.$$

This correlation form was also suggested by Revenga *et al.* [7] with a numerical coefficient that is of the same order of magnitude.

The question whether the function g is indeed independent of $\hat{a} r_c^3/\lambda^3$ awaits future exploration.

ACKNOWLEDGMENTS

This research was supported by the Fund for The Promotion of Research at The Technion, and National Heart, Lung and Blood Institute Grants Nos. NIH HL054885, H1070542, HL074022, and HL075426.

APPENDIX

The equation governing the flow field generated by two rotating, concentric cylinders, in polar coordinates is

$$\frac{\partial v_\theta}{\partial t} = \nu\left(\frac{\partial^2 v_\theta}{\partial r^2} + \frac{\partial v_\theta}{r\partial r} - \frac{v_\theta}{r^2}\right),$$

$$\rho\frac{v_\theta^2}{r} = \frac{\partial p}{\partial r}. \tag{A1}$$

The associated initial and boundary conditions are

$$v_\theta(t=0,r)=0, \quad v_\theta(t,r=r_1)=\omega r_1, \quad v_\theta(t,r=r_2)=\omega r_2. \tag{A2}$$

If Eqs. (A1) and (A2) are rewritten in terms of the dimensionless variables

$$\hat{v}_\theta = v_\theta/\omega r_1, \quad \hat{r}=r/r_1, \quad \hat{\tau}=t\nu/r_1^2, \quad \hat{p}=p/(\rho\omega^2 r_1), \tag{A3}$$

the resulting equations would depend on a single geometrical parameter $R\equiv\hat{r}_2=r_2/r_1$:

$$\frac{\partial\hat{v}_\theta}{\partial\hat{\tau}} = \frac{\partial^2\hat{v}_\theta}{\partial\hat{r}^2} + \frac{\partial\hat{v}_\theta}{\hat{r}\partial\hat{r}} - \frac{\hat{v}_\theta}{\hat{r}^2},$$

$$\frac{\hat{v}_\theta^2}{\hat{r}} = \frac{\partial\hat{p}}{\partial\hat{r}},$$

$$\hat{v}_\theta(\hat{\tau}=0,\hat{r})=0, \quad \hat{v}_\theta(\hat{\tau},\hat{r}=1)=1, \quad \hat{v}_\theta(\hat{\tau},r=\hat{r}_2)=\hat{r}_2. \tag{A4}$$

Notice that, in this case, Eq. (A4) is independent of the physical properties of the liquid.

The general solution for the velocity field can be represented by

$$\hat{v}_\theta = \hat{r} - \hat{u}, \tag{A5}$$

where the first and second terms stand for the steady-state and transient solutions, respectively.

A simple separation of variables leads to the following solution for the transient flow field:

$$\hat{u} = \sum_{n=1}^{\infty} e^{-\lambda_n^2\hat{\tau}}[A_n J_1(\lambda_n\hat{r}) + B_n Y_1(\lambda_n\hat{r})],$$

where

$$A_n = Y_1(\lambda_n)\frac{\int_1^{\hat{r}_2}[J_1(\lambda_n r)Y_1(\lambda_n) - Y_1(\lambda_n r)J_1(\lambda_n)]r^2dr}{\int_1^{\hat{r}_2}[J_1(\lambda_n r)Y_1(\lambda_n) - Y_1(\lambda_n r)J_1(\lambda_n)]^2 rdr},$$

$$B_n = -J_1(\lambda_n)\frac{\int_1^{\hat{r}_2}[J_1(\lambda_n r)Y_1(\lambda_n) - Y_1(\lambda_n r)J_1(\lambda_n)]r^2dr}{\int_1^{\hat{r}_2}[J_1(\lambda_n r)Y_1(\lambda_n) - Y_1(\lambda_n r)J_1(\lambda_n)]^2 rdr}. \tag{A6}$$

Here J_1 and Y_1 are Bessel functions of order 1 of the first and second kind, respectively, and λ_n satisfies the indicial equation

$$J_1(\lambda_n)Y_1(\hat{r}_2\lambda_n) - Y_1(\lambda_n)J_1(\lambda_n\hat{r}_2) = 0, \tag{A7}$$

which depends on a single parameter $\hat{r}_2$ and possesses an infinite countable number of solutions that tend to $\lambda_n \to n\pi/(\hat{r}_2-1)$ for large n's. Figure 5 depicts the velocity distribution for $R=\hat{r}_2=2.1366$ examined in the paper by the DPD method of solution.

[1] P. J. Hoogerbrugge and J. M. V. A. Koelman, Europhys. Lett. **19**, 155 (1992).
[2] P. Espanol and P. B. Warren, Europhys. Lett. **30**, 191 (1995).
[3] A. W. Lees and S. F. Edwards, J. Phys. C **5**, 1921 (1972).
[4] T. Soddemann, B. Dunweg, and K. Kremer, Phys. Rev. E **68**, 046702 (2003).
[5] E. S. Boek, P. V. Coveney, and H. N. W. Lekkerkerker, J. Phys.: Condens. Matter **8**, 9509 (1996).
[6] D. D. Hong, Comput. Mech. **35**, 24 (2004).
[7] M. Revenga, I. Zuniga, P. Espanol, and I. Pagonabarraga, Int. J. Mod. Phys. C **9**, 1319 (1998).
[8] I. V. Pivkin and G. E. Karniadakis, J. Comput. Phys. **207**, 114 (2005).
[9] E. G. Flekkoy and P. V. Coveney, Phys. Rev. Lett. **83**, 1775 (1999).
[10] E. G. Flekkoy, P. V. Coveney, and G. De Fabritiis, Phys. Rev. E **62**, 2140 (2000).
[11] P. Espanol and M. Revenga, Phys. Rev. E **67**, 026705 (2003).
[12] P. Espanol, Phys. Rev. E **57**, 2930 (1998).
[13] A. Malevanets and R. Kapral, J. Chem. Phys. **110**, 8605 (1999).
[14] A. Malevanets and R. Kapral, J. Chem. Phys. **112**, 7260 (2000).
[15] C. A. Marsh and J. M. Yeomans, Europhys. Lett. **37**, 511 (1997).
[16] N. Kikuchi, C. M. Pooley, J. F. Ryder, and J. M. Yeomans, J. Chem. Phys. **119**, 6388 (2003).
[17] M. A. Webster and J. M. Yeomans, J. Chem. Phys. **122**, 164903 (2005).
[18] R. D. Groot and P. B. Warren, J. Chem. Phys. **107**, 4423 (1997).
[19] K. E. Novik and P. V. Coveney, Int. J. Mod. Phys. C **8**, 909 (1997).
[20] G. Besold, I. Vattulainen, M. Karttunen, and J. M. Polson, Phys. Rev. E **62**, R7611 (2000).
[21] M. Revenga, I. Zuniga, and P. Espanol, Comput. Phys. Commun. **121–122**, 309 (1999).
[22] E. Peters, Europhys. Lett. **66**(3), 311 (2004).
[23] I. Vattulainen, M. Karttunen, G. Besold, and J. M. Polson, J. Chem. Phys. **116**(10), 3967 (2002).
[24] A. F. Jakobsen and O. G. Mouritsen, J. Chem. Phys. **122**, 204901 (2005).
[25] T. Ihle and D. M. Kroll, Phys. Rev. E **63**, 020201(R) (2001).